CrossMark

ORIGINAL PAPER

Synthesis, structural and electrical characterizations of LaSrCu$_{0.4}$Al$_{0.6}$O$_{4-\delta}$

B. Negri[1] · M. Leoni[2] · R. Ben Hassen[1]

Abstract A new compound LaSrCu$_{0.4}$Al$_{0.6}$O$_{4-\delta}$ has been prepared by sol gel method, annealed at 1623 K in oxygen gas flow and examined by X-ray diffraction. Rietveld refinement shows that the sample adopts the K$_2$NiF$_4$-type structure, space group I4/mmm ($a = 3.7694(2)$ and $c = 12.8248(5)$ Å, $Z = 2$). Vibrational properties were investigated using Raman scattering and the most characteristic vibrations are discussed with reference to the available structural data. Differential thermal analysis shows two endothermic effects at 329 and 593 K and one exothermic at 693 K. Dielectric study as a function of temperature in the frequency range of 1 kHz–1 MHz has confirmed the observed phase transitions. The value of the measured dielectric constant depends on the frequency and undergoes a large increase near the phase transition temperatures indicating a diffuse behavior of these transitions. Variation of conductivity as a function of temperature shows that the compound has a semiconducting behavior. Oxygen vacancies could be the possible ionic charge carriers. The electrical transport mechanism agrees with Adiabatic Small Polaron Hopping model.

✉ R. Ben Hassen
rached.benhassen@issbat.utm.tn

B. Negri
Negribochra@gmail.com

M. Leoni
matteo.leoni@unitn.it

[1] Unité de Recherche de Chimie des Matériaux et de l'Environnement (UR11ES25), ISSBAT, Université de Tunis El Manar, 9, Avenue Dr. Zoheir Safi, 1006 Tunis, Tunisia

[2] DICAM-University of Trento, via Mesiano, 77, 38123 Trento, Italy

Introduction

Ruddlesden–Popper (RP) phases with the general formula A$_{n+1}$B$_n$O$_{3n+1}$ (A = alkali earth, rare earth elements, B = transition metal cations) are built of n(ABO$_3$) perovskite blocks separated by a single rock salt layer (AO), and are ideal candidates for layer-by-layer assembly. They have attracted a lot of attention in various areas of materials science. Some of the cuprates containing RP phases with $n = 1$ (also known as K$_2$NiF$_4$ type structure) exhibit superconducting properties, for example the cuprates of lanthanum and strontium La$_{2-x}$Sr$_x$CuO$_{4-\delta}$ with composition x(Sr) < 0.26 [1, 2]. Oxygen defect K$_2$NiF$_4$-type oxides La$_{2-x}$Sr$_x$CuO$_{4+-\delta}$ are produced by heterovalent substitution of lanthanum by strontium for a wide composition range: $0 \leq x$(Sr) ≤ 1.34. Three domains have been characterized: orthorhombic compounds for $0 \leq x$(Sr) ≤ 0.1, tetragonal oxides for $0.10 \leq x < 1$ and several superstructures (ref oxygen defect) for $1 \leq x$(Sr) ≤ 1.34. The compounds corresponding to $0 < x < 1$ are characterized by the presence of copper with two oxidation states: $+2$ and $+3$ [3, 4]. The tetragonal modification (space group I4/mmm) is stable for x(Sr) ≥ 0.15 at room temperature and the coordination polyhedra of Cu are distorted octahedra, which are elongated in the axial direction due to the Jahn–Teller effect (d^9 configuration of Cu^{2+}). The oxygen nonstoichiometry of the tetragonal form of La$_{2-x}$Sr$_x$CuO$_{4-\delta}$ is due to an elimination of oxygen, while extra

interstitial oxygen causes the nonstoichiometry in the orthorhombic modification [5].

For the compounds with the composition $x(Sr) > 0.3$, they attracted keen attention due to their high mixed electronic ionic conductivity [6, 7] and they are widely used as electrode materials for fuel cells [8]. The cation composition and the oxygen nonstoichiometry δ influence on their physical and chemical properties. In some cases, such oxygen-deficiency causes modulation in the RP structure as in $LaSrCuO_{3.52}$ [9].

For the anion-deficient $LaSrCuO_{4-\delta}$, the total conductivity at 773 K was 10 S cm^{-1} in air and 1 S cm^{-1} in argon [3, 10] and the conduction becomes of the metal nature at $\sim$ 670 K [3]. Thus, it could be considered as a promising cathodic material for solid-state fuel cells operating in the temperature interval from 800 to 1000 K. On the other hand, the tetragonal $LaSrAlO_4$ with the K2NiF$_4$ structure [11] which has $\varepsilon = 17$, $\tan\delta = 8 \times 10^{-4}$ at 10 GHz, is well distinguished for his very low dielectric loss at microwave frequencies, and has been widely used as high temperature superconducting film (HTSC) substrate [12].

The temperature dependence of the DC electrical conductivity of $LaSrAlO_4$ in air showed linear behavior with a positive temperature coefficient in the temperature range of 750–950 °C. The conductivity was low $(10^{-4}$ S cm$^{-1})$ making the measurements at lower temperatures rather difficult. $LaSrAlO_4$ is an n-type conductor at low oxygen partial pressures and a p-type conductor at near atmospheric pressures [13]. To date, keen attention is drawn to oxide materials with high mixed conduction (electronic and ionic), which hold much promise as the cathodes in intermediate temperature fuel cells. This is the reason why we are more and more interested by mixed oxides based on rare earth and transition metals [14–17]. Thus, we decided to synthesize the new $LaSrAl_{0.6}Cu_{0.4}O_{4-\delta}$ compound by substituting the mixed valence transition metal (Cu) in $LaSrCuO_{4-\delta}$ with a fixed valent cation (Al^{3+}). The main goal of our investigations on these kinds of oxides is to find appropriate compositions with the best set of necessary properties, opening a way for fabricating innovating and high-performance components for application as electrode in solid oxide fuel cells (SOFCs), operating at intermediate temperatures.

Materials and methods

The solid solution of the $LaSrAl_{0.6}Cu_{0.4}O_{4-\delta}$ was prepared using sol–gel method; stoichiometric quantities of La$_2$O3 (99.99%, Aldrich), calcined in air at 1173 K to remove adsorbed water and carbon dioxide, SrCO$_3$ (99.99%, Aldrich), Al(NO$_3$)$_3$·9H$_2$O (98%, Aldrich) and CuO (99.99%, Aldrich) as appropriate, were dissolved in a minimum quantity, typically 150 ml of a 1:2 solution of acetic acid and distilled water. Then, 5 ml of ethylene glycol (99.99%, Aldrich) and one equivalent of citric acid per mole of M^{3+} cation (99.99%, Aldrich) were added and the solution was heated at 353 K with constant stirring for approximately 6 h. Ethylene glycol (HOCH$_2$CH$_2$OH), in this case, does not only act as a complexing agent to form a polymer network, but also to change the distance between the metal ions, which prevents the formation of aggregates of particles of metaloxides during the step elimination of organic compounds. The transparent gel thus formed was decomposed by further heating at 523 K for approximately 3 h. The resulting fine brown powder was ground, and then returned to the furnace in air at 1173 K for 6 h. It is worth known that these synthesized oxides could exhibit semimetallic or metallic properties, in agreement with the existence of the mixed valence Cu(II)–Cu(III). Moreover, those latter properties vary with the oxygen content, i.e., with the method of synthesis [34]. Therefore, the obtained powder was pressed into 13 mm diameter pellets and annealed for 12 h at 1273 K under an oxygen flow in order to intercalate oxygen. The sample reacted slowly and in order to achieve full densification, it was repelleted and sintered numerous times at temperatures ranging from 1273 to 1473 K until no further reaction was noticed by powder X-ray diffraction analysis. Typically sintering times of 12 h × 5 were necessary for complete reaction. With the intention of identifying the phase composition and to refine the structural parameters, the sample was examined by X-ray diffraction using a Bruker D8 diffractometer operating with Cu Kα_1/Kα_2 radiation. Data were collected over a 2θ range from 5° to 90°. The pattern matching and Rietveld refinement were performed with the SIEVE+ (ICDD, International Centre for Diffraction Data) and FullProf (Rodriguez-Carvajal, 1990) softwares, respectively.

A differential thermal analysis (DTA) was carried out up to 723 K by Setaram S60/5190 *DTA* thermal analyzer at a heating rate of 5 K min^{-1}. The experiment was performed using a quantity of 15 mg of fresh prepared sample.

The Raman spectroscopy technique was used as a principle element for characterizing the vibrational and coordination sphere of ions and phase transitions. Raman measurements were performed using the 514.5 nm calibration line from an argon ion laser and analyzed using a Horiba Jobin–Yvon HR800 micro-Raman spectrometer equipped with a charge coupled device. An optical microscope was used to focus the incident light as a spot of about 2 µm in diameter on the sample. Depolarized Raman spectra were obtained in backscattering geometry.

Electrical direct current resistivity measurements were carried out on sintered pellets using a Lucas Labs 302 four

point probe with a Keithley 2400 digital Source Meter (Keithley Instruments, Inc., Cleveland, Ohio). Measurements were performed in the temperature range 293–703 K.

To measure the dielectric properties, silver electrodes are prepared by sputtering on the relevant faces of sintered disk. The relative dielectric permittivity (ε) and dielectric loss ($\tan\delta$) were measured as parametric functions of frequency vs. temperature in the range 300–723 K and frequency from 1 kHz to 1 MHz using a liquid nitrogen cryostat and an HP4284 impedance analyzer interfaced with a PC.

Results and discussion

Structural study

The exact temperature, the gas atmosphere and the duration of reaction were found to be crucial in obtaining pure phase containing no traces of the starting materials. In fact the LaSrAl$_{0.6}$Cu$_{0.4}$O$_{4-\delta}$ sample has been successfully synthesized under flowing oxygen at 1573 K. The purity was verified by a pattern matching performed with the SIEVE+ (ICDD, International Centre for Diffraction Data).

The X-ray diffractogram (Fig. 1) is characterized by the existence of a system of strong peaks, involving the existence of a tetragonal cell. In addition, weak peaks with variable intensities were observed which could not be indexed in this cell. They are suspected to be originated from a superstructure as demonstrated in the border compound LaSrCuO$_{3.52}$ [9]. An electron microscopic study is in progress to confirm this finding. Therefore, a monophasic Rietveld refinement was applied for the LaSrA$_{l0.6}$Cu$_{0.4}$O$_{4-\delta}$ sample by FULLPROF program, using reflections associated to tetragonal cell. The refinement showed a good fit between observed and calculated patterns, and cell dimensions obtained from this refinement are given in Table 1.

According to the Goldschmidt tolerance factor [18], the K$_2$NiF$_4$ type structure is stable over the range $0.866 \leq t < 1$. The T (tetragonal) structure exists for $0.88 \leq t \leq 0.99$ and the T/O (tetragonal/orthorhombic) structure is present for $0.866 \leq t < 0.88$. In general, the closer the tolerance factor of Goldschmidt is to 1, the more the structure is tetragonal (and stable).

For substituted sites, some size averaging is necessary, as done, e.g., by Ganguly et al. [18] for a strontium cuprate with Er^{3+} doping in site A and Ni^{3+} doping in the Cu^{2+}. In our case, we used a weighted average of the Shannon radii of the elements occupying the A and B sites, respectively. The results in Table 1 indicate that by substituting a quantity of aluminum by copper in the system we observe a decrease in the stability (decrease of the Goldschmidt t)

Fig. 1 Observed, calculated and difference profiles for Rietveld refinement of LaSrCu$_{0.4}$Al$_{0.6}$O$_{4-\delta}$ compound
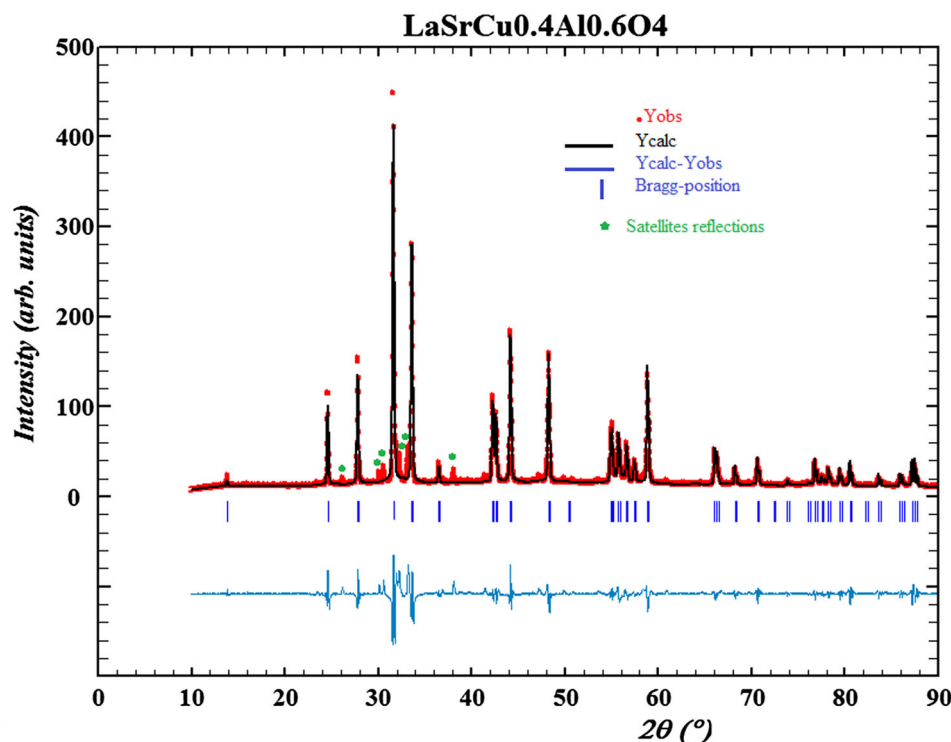
Table 1 Crystallographic parameters for LaSrCu$_{1-x}$Al$_x$O$_{4-\delta}$ ($x = 0$, 0.4, 1)

Specimen	(x)	a Å	c Å	V_{cell} Å^3	V_{ion}	IFF	t	Distort
LaSrCu$_x$Al$_{1-x}$O$_{4-\delta}$	0	3.7553	12.6566	178.49	58.1038	0.6510	0.9157	1.0987
	0.4	3.7694	12.8248	182.22	58.4323	0.6449	0.8784	1.1567
	1	3.7710	13.0325	185.34	59.0919	0.6376	0.8319	1.2469

and an increase in the distortion of the B site octahedra (distortion, calculated as the ratio of the apical vs equatorial oxygen bond lengths moves away from 1). In fact, an elongation in the axial direction is observed due to the Jahn–Teller effect (d^9 configuration of Cu^{2+}) (see Table 3 and Fig. 2).

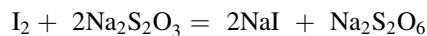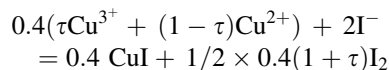It is also interesting to evaluate the ionic filling fraction (IFF) [19], IFF $= V_{ion}/(V_{unit}/Z)$ where V_{ion} is the volume occupied by all ions and Z is the number of formula units. The value calculated (cf. Table 1) is close to that observed by Saato et al. (IFF = 0.69) [19] for a large number of ionic compounds; according to the same author, values lower than 0.69 denote less compact structures that might therefore have an enhanced ionic conductivity.

The structural refinement was carried out in the space group I4/mmm starting with atomic positions taken from LaSrAlO$_4$ [20], with La/Sr and O(2) atoms situated at special positions 4e with coordinates (0, 0, z). The Al and Cu atoms are located at (0, 0, 0) in 2a site, and the O(1)

Fig. 2 Representation of the tetragonal K$_2$NiF$_4$-type structure of LaSrCu$_{0.4}$Al$_{0.6}$O$_{4-\delta}$ compound showing the octahedral coordination around the Cu/Al and the layered nature of the structure

atoms at (0, ½, 0) in 4c site. Atomic positions have been refined for all the atoms, together with scale factor and profile parameters. It is well known that in Rietveld refinements of heavy-atom structures, using X-ray diffraction data, much problematic intensity may be hidden in the thermal displacement factors of relatively light atoms. That is why we have undertaken the refinement of oxygen atoms with fixed occupancies at 1 and thermal displacement factors fixed at values higher than those of heavy atoms. This tendency makes it impossible to locate the oxygen vacancies, which creates a doubt in the determination of oxygen environments for Cu/Al atoms, leaving the possibility only for an octahedral environment. Refinements of the physically sensible isotropic temperature factors were unstable, but good results were obtained by refinement of overall isotropic displacement factor. Finely refinement of the preferred orientation correction in the [004] direction led to a highly significant diminution of χ^2, and a considerable improvement in the visual quality of the fit. A final refinement converged to the structural parameters given in Tables 2 and 3.

Chemical analysis

Iodometric titration was used for the determination of the average copper oxidation state and copper content in the sample. To determine the copper oxidation state, a powdered sample of nearly 0.01 g was taken, and dissolved under stirring in HCl solution 6 M leading to reduction of all the copper ions (Cu^{3+} and Cu^{2+}), to Cu$^+$ ion. Then, 10 ml of 20% KI was added. The formed iodine was titrated with a defined volume V of sodium thiosulfate Na$_2$S$_2$O$_3$ standard solution.

$$0.4(\tau Cu^{3+} + (1-\tau)Cu^{2+}) + 2I^-$$
$$= 0.4\ CuI + 1/2 \times 0.4(1+\tau)I_2$$

$$I_2 + 2Na_2S_2O_3 = 2NaI + Na_2S_2O_6$$

The oxygen nonstoichiometry (δ) is directly correlated with the Cu^{3+} content according to the formulation: LaSrAl$_{0.6}$(Cu^{3+}$_\tau$Cu^{2+}$_{1-\tau}$)$_{0.4}$O$_{4-\delta}$.

The titration of the resulting I$_2$, by a solution of Na$_2$S$_2$O$_3$ sodium thiosulfate, led to determining the value $\tau = 0.0154$ and therefore $\delta = 0.203$. The obtained results indicate that the compound is oxygen deficient.
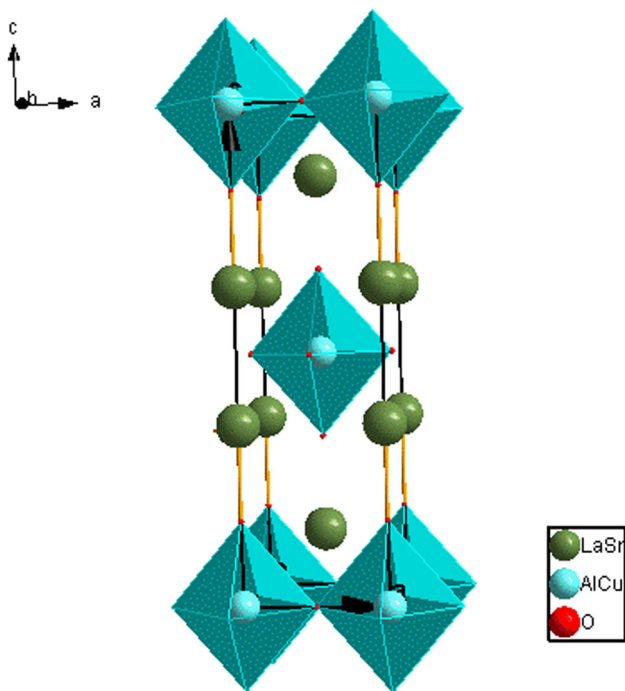
Table 2 Crystallographic data of $LaSrCu_{0.4}Al_{0.6}O_{4-\delta}$ and structural parameters of $LaSrCu_{0.4}Al_{0.6}O_{4-\delta}$ obtained from Rietveld refinements of powder XRD data

Chemical composition	$LaSrCu_{0.4}Al_{0.6}O_{4-\delta}$				
Space group	I4/mmm				
a Å	3.7694 (2)				
c Å	12.8248 (5)				
V Å^3	182.2176 (1)				
D_x (g cm^{-3})	6.054				
Atoms	Wyckoff positions	x	y	z	Occ
La/Sr	4e	0	0	0.3620 (2)	0.5/0.5
Cu	2a	0	0	0	0.4
Al	2a	0	0	0	0.6
O_2	4e	0	0	0.1708 (3)	1
O_1	4c	0	1/2	0	1
R factors	(%)				
R_{Bragg}	16.7				
Rp	9.6				
Rwp	15.8				
Rf	12.2				
χ^2	0.615				

Table 3 Inter-atomic distances (Cu/Al)–O and (La/Sr)–O for $LaSrCu_{0.4}Al_{0.6}O_{4-\delta}$

Cu/Al–O (in-plane) (Å)	1.8847 (1)
Cu/Al–O (apical) (Å)	2.1907 (2)
La/Sr–O (Å)	2.4527 (4)

Thermal analysis

The behavior of the phase transitions in $LaSrAl_{0.6}Cu_{0.4}O_{4-\delta}$ was analyzed with differential thermal analysis (DTA). These measurements were carried out at a rate of 5 K min^{-1} in the temperature range 299–773 K using 50 mg of $LaSrAl_{0.6}Cu_{0.4}O_{4-\delta}$ powder in a platinum crucible. Figure 3 shows the DTA curves of $LaSrAl_{0.6}Cu_{0.4}O_{4-\delta}$.

We note two endothermic effects at 329 and 593 K and one exothermic at 693 K, where the slope of the change in measurement indicates three consecutive possible phase transitions. The first anomaly at 329 K is clearly manifested in the dielectric data. At 593 and 699 K, the DTA measurement shows two anomalies presented by peaks with different forms, the first one reveals a second-order transition and the second one is of first order. Both effects are identical to those reported in the literature of related compounds $LaSrAlO_4$ and $CaNdAlO_4$ [21]. Authors of this reference indicated that the plausible cause of the first effect may be a second-order phase transition which involves rearrangement of ions in the unit cell. And they suggested that the second observed exothermic effect in the as-grown crystals is explained by oxygen deficiencies in as-grown crystals.

Raman spectroscopy

Despite several Raman studies on Strontium lanthanum cuprate and aluminate as ceramics and single crystals, there is still no agreement on the assignment of their vibrational modes [35]. In addition, other studies on single crystals have shown a strong forbidden line in one case and, in another case, evidence for Raman scattering from antiferromagnetic spin waves, which are two-dimensional correlations in The Cu-0 planes [22, 25]. The presence of such effects certainly further complicates the spectral analysis of polycrystalline samples and among others our $LaSrAl_{0.6}Cu_{0.4}O_{4-\delta}$. We do not intend to detail in our case its vibrational study. We just limit ourselves to highlight the effect of the changes at the levels of polyhedra of coordination on optical phonons due to the substitution of the Cu by the Al. $LaSrAl_{0.6}Cu_{0.4}O_{4-\delta}$ presents a tetragonal crystal structure. A factor-group analysis of the $k \sim 0$ normal modes of the tetragonal structure (D^{17}_{4h}) yields for the Raman-active phonon $2A_1g + 2Eg$ symmetry modes [23, 24]. By analogy with the parent compounds $LaSrCuO_4$ and its homolog $LaSrCuO_4$, these modes are due to the vibrations of the La/Sr and the apex oxygen atoms (A_{1g}) and the tilting octahedral vibrations along the two diagonal axes of the Cu/AlO_2 planes (Eg). We shall not give a detailed assignment here, but we intend as far as possible to distinguish between the bands corresponding to the motions of Al–O octahedra and those associated with Cu–O. The peaks associated with the vibrations of the apical oxygen atoms along the c axis are observed at the region between 425 and 439 cm^{-1} [22, 23]. In addition, a lower frequency band at 160 cm^{-1} is assigned by analogy with $LaSrAlO_4$ to La/Sr vibrations in the *ab*-plane [25] and those at the region between 291 and 313 cm^{-1} to the same type of vibration of oxygen atoms, as mentioned in the literature [26]. It seems that we have succeeded to indicate all the Raman phonon allowed by symmetry.

The Raman spectra of polycrystalline sample of $LaSrAl_{0.6}Cu_{0.4}O_{4-\delta}$ are remarkable. First, the intensities of peaks associated with vibrations of the apical oxygen atoms along the *c* axis and to the motion of the La/Sr atoms in the *ab* plane at, respectively, 439 and 160 cm^{-1} are very weak and presented as broad width. Second, a lot of extra peaks appeared at 263, 321, 373, 557 and 630 cm^{-1} are

Fig. 3 Differential thermal analysis (DTA) of LaSrCu$_{0.4}$Al$_{0.6}$O$_{4-\delta}$ at elevated temperatures
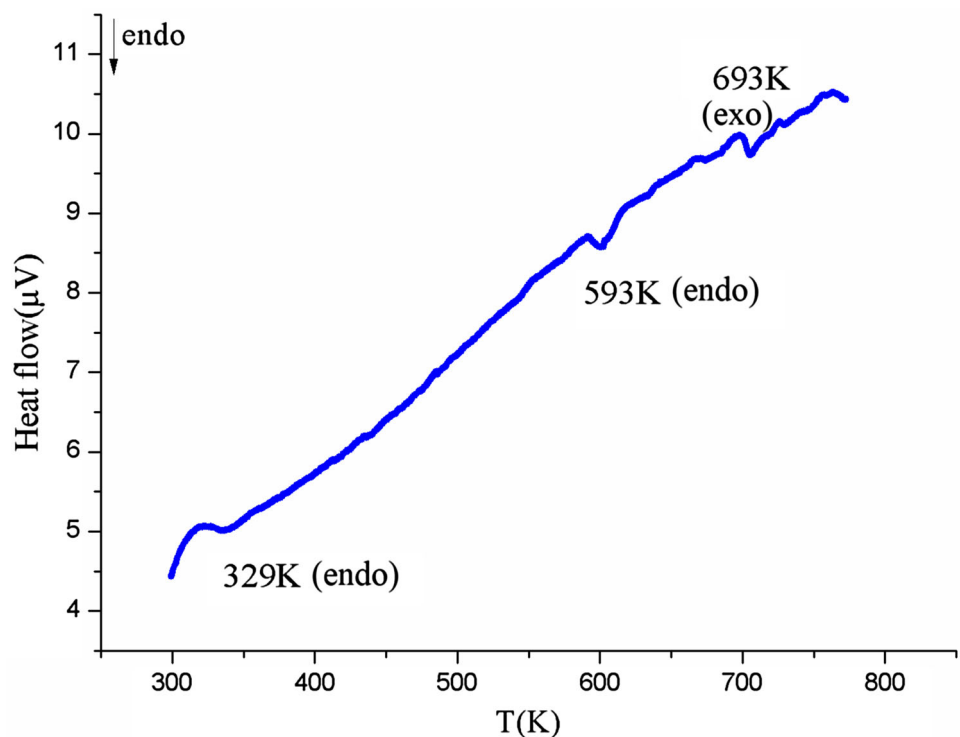
indicated in the literature as forbidden modes [26]. The remaining should be related to changes in coordination and the existence of two kinds of polyhedra Cu–O and Al–O. It is possible that defects such as vacancies could result in such observable scattering. All the collected Raman spectra are presented as wide and unresolved bands indicating a big degree of disorder. This behavior has been attributed to the Cu-induced disorder which results in a displacement of the apex atom from equilibrium to an interstitial position. The observed phenomena could also involve other mechanisms such as a redistribution of the charges. The spectral changes with temperature increase are illustrated in Fig. 3. These changes are related to the internal vibrations of the Cu–O and Al–O polyhedra, as well as external vibrations (lattice modes) and relate to all the observed phase transitions. These latter are defined by the following modifications:

- The 160 cm^{-1} band associated with La/Sr vibrations in the *ab*-plane broadens to 344 K (after the first transition) and then becomes narrow and shifts towards 193 cm^{-1} to 603 K (third transition) and eventually disappears at 703 K after the fourth transition.
- An increasing in the width of the band at 372 cm^{-1} at temperature T = 603 K, this can be attributed to the distortion of Cu–O and Al–O polyhedra. Then, at 703 K it vanishes totally.
- The peak at 557 cm^{-1} appears at 603 K and increases with temperature to become well resolved.

- A remarkable reduction in the intensity of the as-called "forbidden band" at 630 cm^{-1} after each transition to almost disappears at 703 K (Fig. 4).

Electrical transport properties

To obtain dense ceramic pellets for electrical measurements, a powder sample of the material was grounded (in ethanol). A pellet (13 mm in diameter and 1.6 mm thick) was prepared by uniaxial pressing (100 MPa). It was then sintered at 1173 K for 4 h to obtain a disk with high density. Using the four-probe technique, the electrical conductivity σ of the sintered ceramic was determined under air in the temperature range of 293–703 K. Figure 5 shows variation of Ln(σT^{α}) versus 1000/T for temperature range of 293–703 K. The increase of Ln(σT^{α}) with increasing temperature indicates that the compound presents a semiconducting behavior over the temperature range 293–703 K. We tried to use the thermal activated small polaron hopping as conduction model [27–30]:

$$\sigma = \sigma_0 T^{-\alpha} \exp\left(\frac{-E_a}{k_B T}\right)$$

where E_a is the activation energy (polaron formation and hopping energy), σ_0 is a constant related to polaron concentration and diffusion, in the above Arrhenius equation, $\alpha = 1$ corresponds to a small adiabatic polaron hopping and $\alpha = 1.5$ in the case of a small non-adiabatic polaron

hopping. In the analysis of the simulated curve Ln(σ T^α) = f (1000/T), we found that the convergence of the curve fitting is reached throughout all the temperature ranges and that the best fit is observed for a value of $\alpha = 1$. This suggests that the charge transport in the LaSrAl$_{0.6}$Cu$_{0.4}$O$_{4-\delta}$ is described by a model of small adiabatic polaron hopping in all the temperature zones, with different energies of activation. The fitting parameters σ_0 and E_a are $\sigma_{0(1)} = 12.13\ \Omega^{-1}\ m^{-1}$ and $E_{a(1)}$ 0.54 eV, respectively, for temperature range 293–329 K, $\sigma_{0(2)} = 73.61\ \Omega^{-1}\ m^{-1}$ and $E_{a(2)} = 0.78$ eV for temperature range 329–434 K and $\sigma_{0(3)} = 7.44 \times 10^{-4}\ \Omega^{-1}\ m^{-1}$ and $E_{a(3)} = 0.32$ eV for temperature range 434–590 K, $\sigma_{0(4)} = 6.63 \times 10^{-4}\ \Omega^{-1}\ m^{-1}$ and $E_{a(4)} = 0.13$ eV for temperature range 590–699 K, $\sigma_{0(5)} = 0.16\ \Omega^{-1}\ m^{-1}$ and $E_{a(5)} = 0.22$ eV for temperature range 699–703 K.

By comparing the results found by Mazo et al. in their work on LaSrCuO$_{4-\delta}$ [3], one can notice that:

a.　The conductivity again increases with the heating up to $T \sim 699$ K, but the values observed in our sample are much smaller.

b.　The transition from a semiconductor (p type) to a metal, observed in LaSrCuO$_{4-\delta}$ [3], is probably shifted to a higher temperature, in our case.
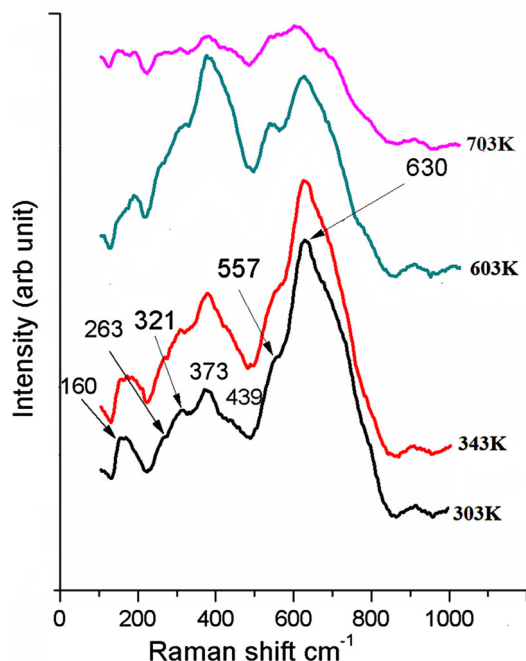
Fig. 4 Temperature dependence of Raman spectra for LaSrCu$_{0.4}$Al$_{0.6}$O$_{4-\delta}$

Dielectric studies

Figures 6 and 7 show the temperature dependence of the dielectric constant and dielectric loss at various frequencies. For all measured frequencies, we find unambiguous subtle anomalies in the dielectric constant and dielectric loss. We see that $\varepsilon'(T)$ and tan(δ) behave like plates independent of frequency and temperature less than $T = 350$ K. This is the intrinsic dielectric response of electronic and/or ionic polarizations. When the temperature above 350 K, a stepwise increase in $\varepsilon'(T)$ occurs. It can be seen that the curves tan(δ) increased rapidly with increasing temperature.

LaSrAl$_{0.6}$Cu$_{0.4}$O$_{4-\delta}$ displays two dielectric constant peaks, identified by a high-frequency dispersion in the vicinity of each peak, a decrease in the value of the permittivity as a function of frequency and, a shift of the temperatures (Tm) corresponding to maximum value of the dielectric constant towards higher temperatures when decreasing the frequency. The maximum values of the dielectric constant are observed at the vicinity of Tm$_1$ = 538 K and Tm$_2$ = 598 K for frequency of 1000 Hz. We note that the first observed anomaly at Tm$_1$ = 538 K for 1000 Hz has not been detected by DTA analysis; however, the second anomaly at Tm$_2$ = 598 K corresponds well to the 2nd phase transition already signaled above.

The high observed value of ε' at low frequency for all temperatures may be due to the presence of different types of polarization (i.e., electron, dipole, interfacial, ionic orientation, etc.) [31, 32]. In addition, the decrease in ε' with increasing frequency (Fig. 5) is a typical characteristic of dielectric materials and can be attributed to the fact that in the low frequency regions the permanent dipoles align along the direction of the field and contribute to the total polarization of the dielectric material.

The comparison with the parent compound LaSrAlO$_4$ shows the absence of any significant background and the total disappearance of relaxation which was exclusively associated with conductivity as mentioned by Zhang et al. [33].

Conclusion

LaSrAl$_{0.6}$Cu$_{0.4}$O$_{4-\delta}$ was successfully synthesized by sol–gel at relatively low temperatures in comparison with conventional solid-state methods. Electrical conductivity studies were carried out as a function of temperature. The conductivity values observed in our sample are much lower than those observed in LaSrCuO$_4$ and higher than those in LaSrAlO$_4$. The transition from a semiconductor (type p) to a metal, already observed in LaSrCuO$_4$, is probably

Fig. 5 Arrhenius relations of $Ln(\sigma T^{\alpha})$ versus 1000/T for the $LaSrCu_{0.4}Al_{0.6}O_{4-\delta}$
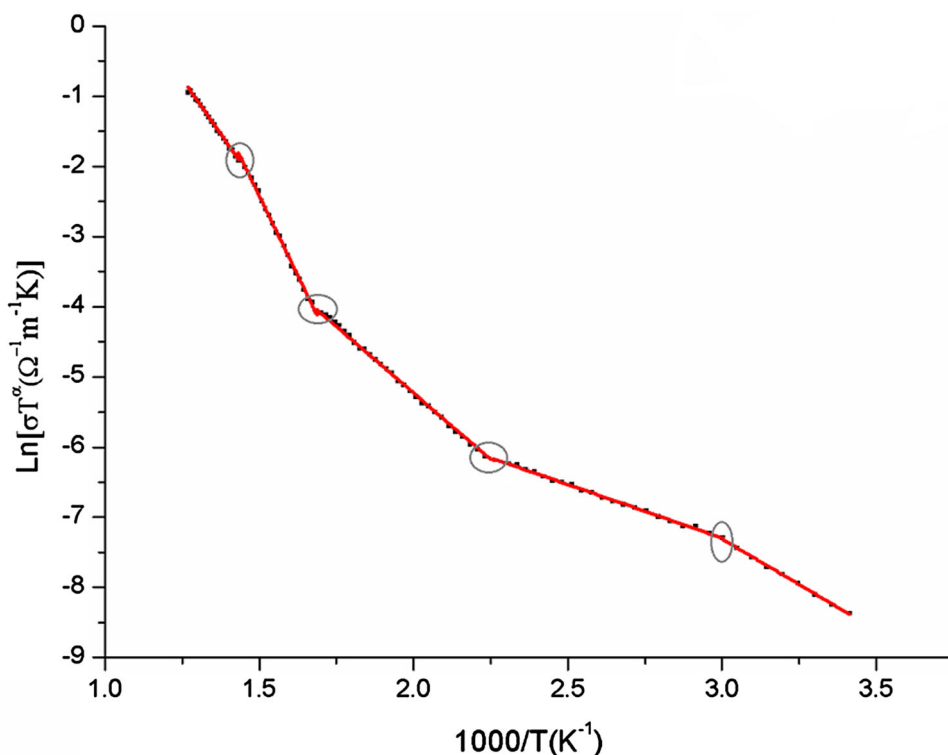

Fig. 6 Thermal variation of the real permittivity (ε') for $LaSrCu_{0.4}Al_{0.6}O_{4-\delta}$ compound
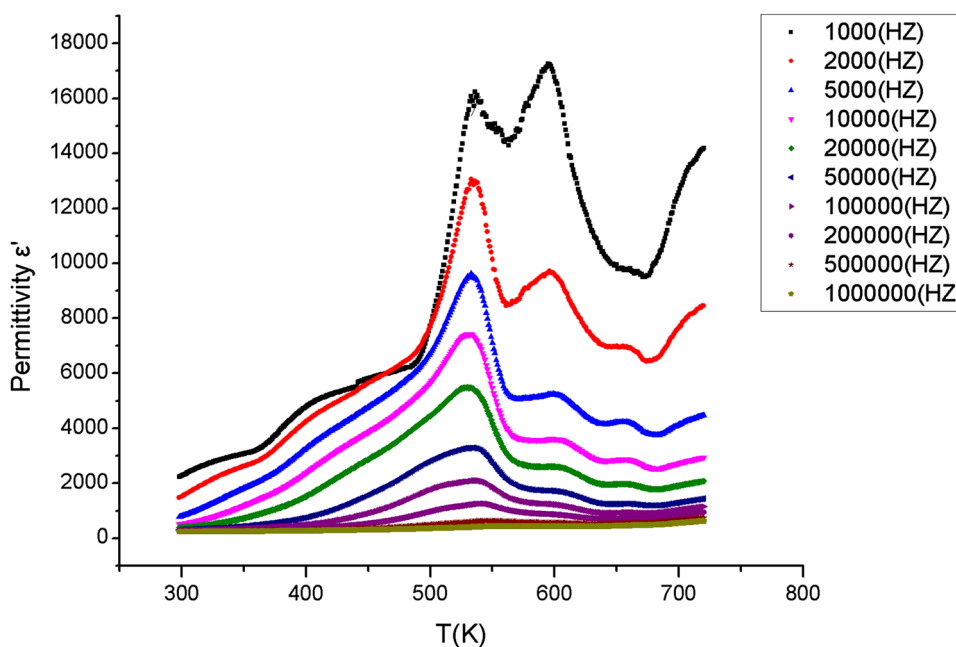
disappeared or shifted at a higher temperature in our case. The conduction mechanism corresponds to the thermal activated small adiabatic polaron hopping. In the as-prepared sample, the dielectric behaviors are consistent with those of $LaSrAlO_4$ [33] and can be interpreted in terms of the hopping motion of polarized clusters created by the holes. $LaSrAl_{0.6}Cu_{0.4}O_{4-\delta}$ sample shows intrinsic

dielectric behavior at temperatures below ~ 350 K and giant dielectric behavior is observed in the temperature range above ~ 350 K. This behavior is mainly contributed by the bulk effect due to hopping motions of oxygen vacancies in the temperature range of 350–720 K. Three phase transitions at 329, 593 and 693 K characterized by
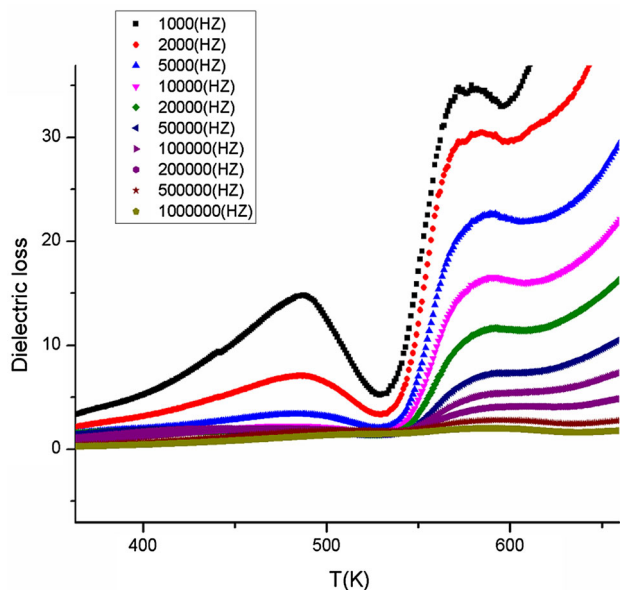
Fig. 7 Dielectric loss (tanδ) for LaSrCu$_{0.4}$Al$_{0.6}$O$_{4-\delta}$ compound

differential thermal analysis (DTA) were confirmed by Raman scattering and electrical conductivity analysis.

References

1. Shafer, M.W., Penney, T., Olson, B.L.: Correlation of Tc with hole concentration in La$_{2-x}$Sr$_x$CuO$_{4-\delta}$ superconductors. Phys. Rev. B. **36**, 4047 (1987)
2. Torrance, J.B., Yokura, T., Nazzal, A.I., Bezinge, A., Huang, T.C., Parkin, S.S.: Anomalous disappearance of high-Tc superconductivity at high hole concentration in metallic La$_{2-x}$Sr$_x$CuO$_4$. Phys. Rev. Lett. **61**, 1127 (1988)
3. Mazo, G.N., Savvin, S.N., MychkaYu, E.V., Dobrovol'skii, A., Leonova, L.S.: Conductivity of lanthanum–strontium cuprate LaSrCuO$_{4-\delta}$ and ionic reversibility of relevant electrodes. Russ. J. Electrochem. **41**, 448–454 (2005)
4. Zipprich, W., Wiemhofer, H.D.: Measurement of ionic conductivity in mixed conducting compounds using solid electrolyte microcontacts. Solid State Ionics **135**, 699 (2000)
5. Kharton, V.V., Marques, F.M.B.: Mixed ionic–electronic conductors: effects of ceramic microstructure on transport properties. Curr. Opin. Solid State Mater. Sci. **6**, 261 (2002)
6. Kharton, V.V., Viskup, A.P., Naumovich, E.N., Marques, F.M.B.: Oxygen ion transport in La$_2$NiO$_4$-based ceramics. J. Mater. Chem. **9**, 2623 (1999)
7. Shilova, Y.A., Patrakeev, M.V., Mitberg, E.B., Leonidov, I.A., Kozhevnikov, V.L., Poeppelmeier, K.R.: Order–disorder enhanced oxygen conductivity and electron transport in Ruddlesden Popper ferrite–titanate Sr$_3$Fe$_{2-x}$Ti$_x$O$_{6+\delta}$. J. Solid State Chem. **168**, 275 (2002)
8. Mazo, G.N., Savvin, S.N., Abakumov, A.M., Hadermann, J., Dobrovol'skii, Y.A., Leonova, L.S.: Lanthanum–strontium cuprate: a promising cathodic material for solid oxide fuel cells. Elektrokhimiya **43**, 436–442 (2007)
9. Hadermann, J., Perez, O., Creon, N., Michel, C., Hervieu, M.: The $(3 + 2)$D structure of oxygen deficient LaSrCuO$_{3.52}$. J. Mater. Chem. **17**, 2344–2350 (2007)
10. Yu, H.C., Fung, K.Z.: La$_{1-x}$Sr$_x$CuO$_{2.5-\delta}$ as new cathode materials for intermediate temperature solid oxide fuel cells. Mater. Res. Bull. **38**, 231–239 (2003)
11. Pajaczkowska, A., Gloubokov, A.: Synthesis, growth and characterization of tetragonal ABCO$_4$ crystals. Prog. Cryst. Growth Charact. Mater. **36**, 123 (1998)
12. Matsushima, Y., Ishizawa, N., Kodama, N.: Synchrotron X-ray and molecular dynamics studies of CaYAlO$_4$: the role of heterovalent solutes in K$_2$NiF$_4$-type solid solutions. Phys C. **338**, 166 (2000)
13. Raj, E.S., Skinner, S.J., Kilner, J.A.: Solution synthesis and electrical properties of K$_2$NiF$_4$ type LaSrAlO$_4$. Solid State Sci. **6**, 825–829 (2004)
14. Chaker, H., Roisnel, T., Potel, M., Hassen, R.B.: Structural and electrical changes in NdSrNiO$_{4-\delta}$ by substitute nickel with copper. J. Solid State Chem. **177**, 4067–4072 (2004)
15. Jammali, M., Chaker, H., Cherif, K., Hassen, R.B.: Investigation on the structural and electrical properties of NdSrNi$_{1-x}$Cr$_x$O$_{4+\delta}$ $(0.1 < x < 0.9)$ system. J. Solid State Chem. **183**, 1194–1199 (2010)
16. Hamdi, S., Ouni, S., Chaker, H., Rohlicek, J., Hassen, R.B.: Synthesis, structural and electrical characterizations of DySr$_5$Ni$_{2.4}$Cu$_{0.6}$O$_{12-\delta}$. J. Solid State Chem. **184**, 2897–2901 (2011)
17. Hamdi, S., Ouni, S., Chaker, H., Hassen, R.B.: Synthesis structural and electrical characterizations of Er$_{0.33}$Sr$_{1.67}$Ni$_{0.8}$Cu$_{0.2}$O$_{4-\delta}$. Powder Diffr. **27**, 252–255 (2012)
18. Ganguly, P., Rao, C.N.R.: Crystal chemistry and magnetic properties of layered metal oxides possessing the K$_2$NiF$_4$ or related structures. J. Solid State Chem. **53**, 193–216 (1984)
19. Sato, T., Takagi, S., Deledda, S., Hauback, B.C., Orimo, S.I.: Extending the applicability of the Goldschmidt tolerance factor to arbitrary ionic compounds. (2016). Scientific Reports, doi:10.1038/srep23592
20. Fan, X.C., Chen, X.M., Liu, X.Q.: Structural dependence of microwave dielectric properties of SrRAlO$_4$ (R = Sm, Nd, La) ceramics: crystal structure refinement and infrared reflectivity study. Chem. Mater **20**, 4092–4098 (2008)
21. Byszewskiab, P., Domagala, J., Fink-Finowicki, J., Pajaczkowska, A.: Thermal properties of CaNdAlO$_4$ and SrLaAlO$_4$ single crystals. Mater. Res. Bull. **27**, 483–490 (1992)
22. Weber, W.H., Peters, C.R., Logothetis, E.M.: Raman studies of lanthanum cuprate superconductors. J. Opt. Soc. Am. B **6**, 455–464 (1989)
23. Sugai, S., Uchida, S., Takagi, H., Kitazawa, K., Tanaka, S.: Infrared spectroscopy in high Tc superconductors (La$_{1-x}$Sr$_x$)$_2$CuO$_4$. Jpn. J. Appl. Phys. **26**, L879–L881 (1987)
24. Burns, G., Chandrashekhar, G.V., Dacol, F.H., Shafer, M.W.: Raman measurements of the superconductor (La$_{2-x}$Sr$_x$)CuO$_4$. Solid State Commun. **68**, 67–69 (1988)
25. Hadjiev, V.G., Cardona, M., Ivanov, I., Popov, V., Gyulmezov, M., Iliev, M.N., Berkowski, M.: Optical phonons probe of the SrLaAlO$_4$ crystal structure. J. Alloy. Compd. **251**, 7–10 (1997)
26. Rousseau, D.L., Bauman, R.P., Porto, S.P.S.: Normal mode determination in crystals. J. Raman Spectrosc. **10**, 253 (1981)

27. Long, A.R., Pollak, M., Shklovskii, B.: Hopping transport in solids, vol. 207. Amsterdam (1991)
28. Tan, X.Y., Chen, C.L., Jin, K.X., Zhao, S.G., Luo, B.C.: Electrical transport and photo induced properties in $La_{0.7}Sr_{0.3}CrO_3$ thin film. Phys. B **403**, 4050–4052 (2008)
29. Mott, N.F., Davis, E.A.: Electronic processes in non-crystalline materials. Clarendon Press, Oxford (1971)
30. Iguchi, E., Nakatsugawa, H., Futakuchi, K.: Polaronic conduction in $La_{2-x}Sr_xCoO_4$ ($0.25 \leq x \leq 1.10$) below room temperature. J. Solid State Chem. **139**, 176–184 (1998)
31. Austin, I.G., Mott, N.F.: Polarons in crystalline and non-crystalline materials. Adv. Phys. **18**, 41–102 (1969)
32. Sinclair, D.C., West, A.R.: Effect of atmosphere on the PTCR properties of $BaTiO_3$ ceramics. J. Mater. Sci. **29**, 6061–6068 (1994)
33. Zhang, J., Li, Y., Xu, D.Y., Tong, L., Qi, H.C., Wang, C.C.: Low-frequency dielectric properties of $SrLaAlO_4$. Ceram. Int. (2017). doi:10.1016/j.ceramint.2017.01.054
34. Weber, W.H., Peters, C.R., Wanklyn, B.M., Chen, C., Watts, B.E.: Evidence for anisotropic excitonlike enhancement of the Raman scattering from La_2CuO_4. Phys. Rev. B **38**, 917–920 (1988)
35. Raveau, B., Michel, C.: Crystal chemistry and properties of mixed valence copper oxides. Annu. Rev. Mater. Sci. **19**, 319–339 (1989)

Publisher's Note